

Chicxulub crater post-impact hydrothermal activity – evidence from Paleocene carbonates in the Santa Elena borehole

J. E. Escobar-Sanchez*, J. Urrutia-Fucugauchi

Proyecto Universitario de Perforaciones en Océanos y Continentes, Laboratorio de Paleomagnetismo y Paleoambientes, Instituto de Geofísica Universidad Nacional Autónoma de México, Mexico City, Mexico

Received: June 12, 2009; accepted: February 16, 2010,

Resumen

Los cráteres de impacto se caracterizan por sistemas hidrotermales activos; particularmente en aquellos formados en ambientes marinos, en los cuales los procesos convectivos incluyen fluidos hidrotermales y agua de mar. En este estudio se presentan resultados sobre la actividad hidrotermal en el cráter Chicxulub, formado por un impacto sobre la plataforma carbonatada en el sur del Golfo de México hace unos 65 Ma en el límite Cretácico/Terciario. Los sedimentos carbonatados post-impacto registran los efectos de actividad hidrotermal convectiva, lo cual nos permite investigar sobre las características y duración de estos procesos. En este artículo se presentan la geoquímica de elementos mayores y traza de los sedimentos carbonatados correspondientes a la secuencia basal del Paleoceno a una profundidad de 304 a 332 metros en los núcleos del pozo Santa Elena, localizado al sur del borde de la cuenca principal del cráter Chicxulub. La geoquímica de elementos mayores y traza registra evidencias de actividad hidrotermal, marcada por un enriquecimiento en los primeros 10 metros de la secuencia sobre el contacto con las brechas de impacto. Las calizas presentan concentraciones altas de sílice, magnesio, aluminio, potasio y hierro, observándose patrones de variaciones similares en otros óxidos, así como en los elementos traza. El enriquecimiento concuerda con modelos de variación asociados a un aporte hidrotermal mejor que con otros posibles procesos asociados como podrían ser efectos diagenéticos o contribuciones detríticas procedentes de otras fuentes. El contenido relativo de los óxidos mayores en los primeros 12 metros de la sección (desde los 332 hasta los 322 metros), presenta 50 % de CaO y alrededor del 2% de SiO₂ y MgO; patrones similares se observan para los otros óxidos, así como para los elementos traza. Considerando que la posición del sitio de estudio, se encuentra cercana a la zona central, las anomalías geoquímicas, presentan una elevada actividad convectiva provocada por la brecha de impacto subyacente a esta secuencia, y el aporte asociado con las fuentes hidrotermales distales del área central. Las concentraciones de Fe, K y Al corresponden con un aporte hidrotermal, también observado en los elementos traza (Zn, V, Cr, Ni, Cu, Zr y Rb). Después del cese de la actividad mayor hidrotermal, aproximadamente enseguida de 1 Ma posterior al impacto, actividad intermitente hidrotermal posiblemente continuó operando por un periodo mayor.

Palabras clave: Cráter de impacto, sistema hidrotermal, sedimentos carbonatados, cráter de Chicxulub, México.

Abstract

Active hydrothermal systems develop in impact structures formed in marine settings, associated with convective processes involving hydrothermal fluids and seawater. Here we investigate hydrothermal activity in the Chicxulub crater, which was formed by a large impact on the Yucatan carbonate platform in the southern Gulf of Mexico at the Cretaceous/Tertiary boundary. The post-impact cover carbonate sediments carry a record of convective hydrothermal activity, which allow investigating on characteristics and timing/duration of the processes. We present the major and trace element geochemistry of basal Paleocene carbonate sediments (304-332 m depth) in the Santa Elena borehole located south of the crater rim outside of the main basin. Hydrothermal activity is evidenced in the major oxides and trace elements, enriched in the first 10 m above the impact breccia-carbonates contact. Basal limestones present high concentrations of silica, magnesium, aluminum, potassium and iron, with similar variation patterns in the other oxides and the trace element data. The geochemical data are consistent with element enrichment associated with hydrothermal input and less likely to result from other processes like diagenesis or detrital contributions. The relative contents of major oxides remain constant in the next twelve meters of the section above 322 m, with CaO around 50 % wt and SiO₂ and MgO around 2 % wt and similar pattern in other oxides and trace elements. Considering location of the study site away from the central zone, the geochemical anomalies may arise from convective activity on the underlying impact breccia sequence and input to the water column associated with the distal hydrothermal vent sources in the central area. Concentration in Fe, K and Al is suggestive of a step pattern, also observed in the trace elements (Zn, V, Cr, Ni, Cu, Zr and Rb). After cessation of the active hydrothermal phase after ~1 Ma following the impact, intermittent hydrothermal venting may have operated for an extended time.

Key words: Impact craters, hydrothermal systems, carbonate sediments, Chicxulub crater, Mexico.

Introduction

Large impact craters are characterized by hydrothermal systems associated with a thermal anomaly from energy released by the impact, deformation and fracturing of target material, crustal excavation and uplift, and formation of melt sheet and impact breccias. Impacts on marine environments develop long-lived convective hydrothermal systems, where seawater, groundwater, formational brines and magmatic fluids circulate deep in the crust and within the crater lithologies. Craters formed on continental shelf settings like Sudbury, Chicxulub, Siljan, Ries, Puckezh-Kantunki, Kara and others present evidence of hydrothermal alteration in the impact lithologies. The fluid circulation appears related to permeability, porosity, fracturing and crater morphology (e.g., Melosh, 1989; Zurcher and Kring, 2004; Urrutia-Fucugauchi and Perez-Cruz, 2009). Study of hydrothermal systems in geologic settings with sedimentary, igneous and metamorphic rocks in addition to the impact lithologies is a complex task. To study hydrothermal processes, systems formed in simpler settings might provide insights on the characteristics and fluid circulation controls.

We investigate the hydrothermal system in the Chicxulub crater. Chicxulub was formed by a large impact

on the Yucatan carbonate platform in the southern Gulf of Mexico at the Cretaceous/Tertiary (K/T) boundary. The Yucatan platform has not been affected by volcanic and tectonic activity and the crater was covered by carbonate sediments after the impact and crater formation. Studies in the impact breccias sampled in the drilling programs conducted in Chicxulub have successfully documented the hydrothermal activity (e.g., Ames *et al.*, 2004; Kring *et al.*, 2004; Rowe *et al.*, 2004; Zurcher and Kring, 2004). At the time of impact the area was a shallow marine environment, and the crater formed a depositional basin for carbonate sedimentation in the Yucatan platform. The crater is presently covered by up to ~1 km of carbonate sediments. The post-impact basal carbonate sequence carries a record of the convective hydrothermal activity and permits to investigate on characteristics and timing/duration of the processes.

In this paper, we report the results of a study of the Paleocene carbonate basal sequence of Chicxulub, directed to investigate the post-impact hydrothermal activity and its influence in the crater basin and surrounding shallow carbonate platform. We study the cover carbonate sediments sampled in the Santa Elena borehole located close to the crater rim of Chicxulub (Fig. 1).

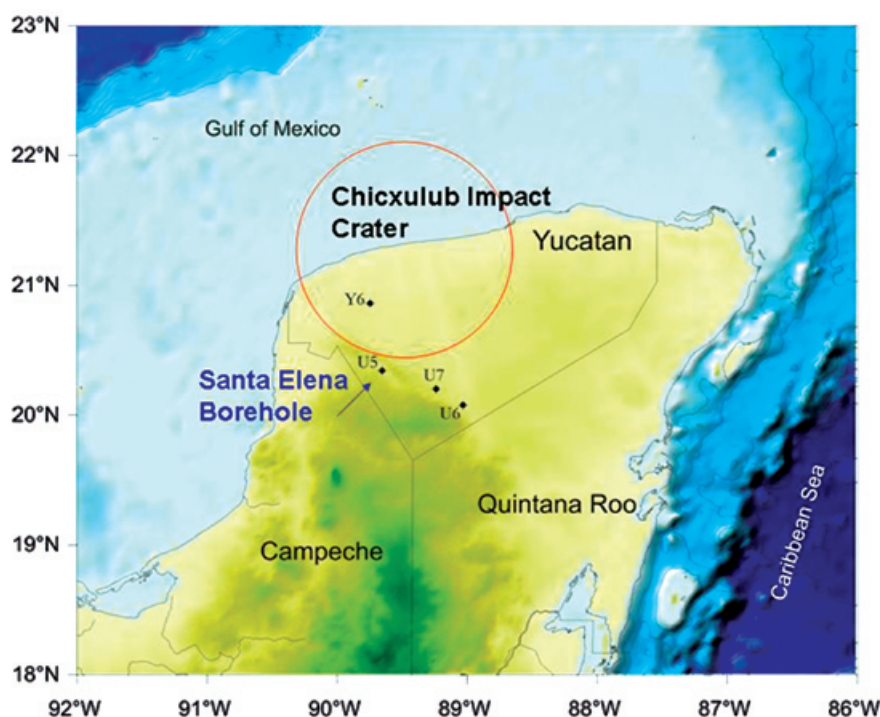


Fig. 1. Schematic map of the Yucatan carbonate platform and Chicxulub crater, showing location of drilling sites (UNAM boreholes U5, U6 and U7) (modified from Urrutia-Fucugauchi *et al.*, 2008). The study is made on samples from the basal Paleocene section in the Santa Elena borehole (U5), located in the southern sector of the crater.

Chicxulub crater UNAM drilling program

Chicxulub crater formed in the shallow extensive platform of the Yucatan peninsula and has been afterwards buried by up to 1 km of Tertiary and Quaternary carbonate sediments. Crater studies have relied on geophysical surveys, which provided the initial indications for its discovery (Penfield and Camargo, 1981; Hildebrand *et al.*, 1991; Sharpton *et al.*, 1992). Gravity, aeromagnetics, magnetotelluric and seismic refraction and reflection surveys have provided high-resolution imagery of the crater in both the offshore and onshore portions, characterizing the impact deposits, cover sediments and deep structure (e.g., Sharpton *et al.*, 1993; Pilkington *et al.*, 1994; Hildebrand *et al.*, 1998; Morgan *et al.*, 1997; Campos-Enriquez *et al.*, 1997; Connors *et al.*, 1996; Delgado-Rodriguez *et al.*, 2001; Urrutia-Fucugauchi *et al.*, 2004a, 2008; Collins *et al.*, 2008; Gulick *et al.*, 2008; Salguero-Hernandez *et al.*, 2010).

Aeromagnetic data show high amplitude short wavelength anomalies in the central sector delineated by the gravity anomalies, associated with the central basement uplift, breccias and melt (Pilkington *et al.*, 1994; Ortiz-Aleman *et al.*, 2001). Structural models derived from modeling the potential field anomalies and electromagnetic data define major crater features, including a central zone with the basement uplift, breccias and melt deposits, and terrace zones with radial faulting. Seismic reflection surveys have allowed mapping and imaging of crater morphology, Tertiary basin and deep crustal deformation features (Morgan *et al.*, 1997). Joint modeling of geophysical data and drilling data, particularly lithological columns and well logging information have resulted in improved spatial resolution and identification of crater units (Hildebrand *et al.*, 1998; Urrutia-Fucugauchi and Perez-Cruz, 2007; Urrutia-Fucugauchi *et al.*, 2004a, 2008). A recent marine seismic reflection survey has provided three-dimensional imaging of the structure with the peak ring, terrace zones, fractures, Tertiary carbonates, impact deposits and basement Mesozoic sequence (Gulick *et al.*, 2008).

Aeromagnetic data over the structure show three strong, well-defined concentric patterns, with a central 40-km diameter zone of high amplitude anomalies. Magnetic anomalies are interpreted to be associated with the melt sheet, upper breccias and central uplift, which present 3-4 orders of magnitude contrasts with the surrounding carbonate units. Results indicate that magnetic sources extend to a radial distance of ~45 km from the center of the structure with average depths ranging between 2 and 4 km. Magnetic anomaly sources in the central uplift zone are located in the range from 3.5 to 8 km depth, with dominant contributions from an

apparent large body forming the structural uplift (Ortiz-Aleman and Urrutia-Fucugauchi, 2010). The magnetic anomalies associated with the impact breccias likely reflect effects of hydrothermal activity, which has been documented in the magnetic mineralogy of the impact breccias (Pilkington *et al.*, 2004; Urrutia-Fucugauchi *et al.*, 2004b). Hydrothermal alteration resulted in formation in the breccias of secondary Fe-Ti oxides. Petrographic and chemical analyses of samples of melt rocks from the Yucatan-6 borehole, which is located closer to the central zone, indicate no significant hydrothermal alteration in the melt (Kring and Boynton, 1992). In contrast, impact breccias in the Yucatan-6 borehole and other boreholes in the crater show evidence of hydrothermal activity, which is related to the fluid circulation in the fractured porous formations.

Drilling conducted as part of the surveys by Pemex, UNAM and CSDP permitted ground confirmation of the buried structure and samples for laboratory analyses. Pemex drilling incorporated only intermittent core recovery and there was need for detailed sampling through the lithological column (Lopez Ramos, 1976; Urrutia-Fucugauchi and Perez-Cruz, 2007). The UNAM drilling program incorporated continuous coring in eight boreholes distributed within and immediately outside the crater rim, with three boreholes cutting the carbonate-impact breccia contact (Urrutia-Fucugauchi *et al.*, 1996; Rebolledo-Vieyra *et al.*, 2000). The three boreholes, corresponding to UNAM-5 (Santa Elena), UNAM-6 (Peto) and UNAM-7 (Tekax) were located in the southern sector at different radial distances from the crater center located at Chicxulub Puerto (Fig. 1).

The boreholes sampled the Tertiary carbonates and the impact breccia sequence, with the carbonate-breccia contact lying at varying depths between 222 m and 332 m, below the surface. Impact breccias are characterized by clasts of carbonates, melt and crystalline basement in a matrix characterized by carbonate-rich and melt-rich components. Two breccia units, compared to the suevitic and Bunte breccias in the Ries crater, have been cored in Chicxulub, where upper breccias are rich in carbonate clasts and lower breccias are rich in melt and basement clasts (Urrutia-Fucugauchi *et al.*, 1996). Proximal ejecta is documented in these boreholes and in drilling in the eastern crater sector in the Merida-Valladolid area (Urrutia-Fucugauchi *et al.*, 2008). Ejecta deposits are exposed in areas to the south in Belice, Chetumal and Campeche.

We analyze the major and trace element geochemistry of the basal Paleocene carbonate sediments in the Santa Elena borehole, which is located south of the crater rim marked by the cenote ring and outside of the main basin.

Santa Elena Borehole and Paleocene Carbonates

The Santa Elena borehole was selected for studying the hydrothermal activity because of the high core recovery rate, continuous coring of the basal carbonate sequence and melt-rich breccias. The borehole is located ~ 110 km radial distance from the crater center with site coordinates of 89.6615° W, 20.3385° N (Fig. 1). The contact of impact breccias and Tertiary carbonates is at 332.0 m deep where the suevitic breccias present a minimum thickness of 146 m. The basal carbonate sequence in the first 30 m above the contact with the impact breccias is characterized by white cream limestones, with several thin clay layers and variable content of clay lenses (Fig. 2). Clay content and spherical evaporitic minerals increase within the middle section.

The basal section up to 329.75 m is composed of gray carbonates with small cream lenses of calcite and dark gray lenses of apparent melted textures. This is covered by about 3 m of light gray limestones with greater relative contents of clay minerals and < 15% porosity, with no micro-veins and rare evaporitic material. Between about 325 and 315 m, the section is characterized by several clay horizons, and abundance of spheroidal evaporitic aggregates. The limestones show color changes, with darker tones and reduced porosity < 10 % and some

micro-veins. Between about 315 and 311 m, section shows larger proportion of clay and evaporitic minerals, with several well defined clay horizons. Between 303 and 311 m, the section is composed of white cream limestones with ~ 15 % porosity and some micro-veins.

To select samples for the geochemical analyses and to further characterize the carbonates, thin sections were prepared for 23 intervals between ~304 and ~332 m. Nine samples were selected for the detailed study, keeping a denser sampling towards the base of the sequence in the first 12 m.

Geochemistry

Major oxides and trace elements were determined by X-ray fluorescence in the Laboratory of Geochemistry (X-Ray Fluorescence), Institute of Geology at UNAM. Samples were prepared for the geochemical analyses by crushing and powdering with an agata mortar. Analytical procedures and details of the instrumentation are described in Lozano *et al.* (2003). Results are summarized in Table 1 for the major elements and in Table 2 for the trace elements. The laboratory standard used for this set of samples was the ES-17Vq; the analytical data for major oxides and trace elements are included in the tables.

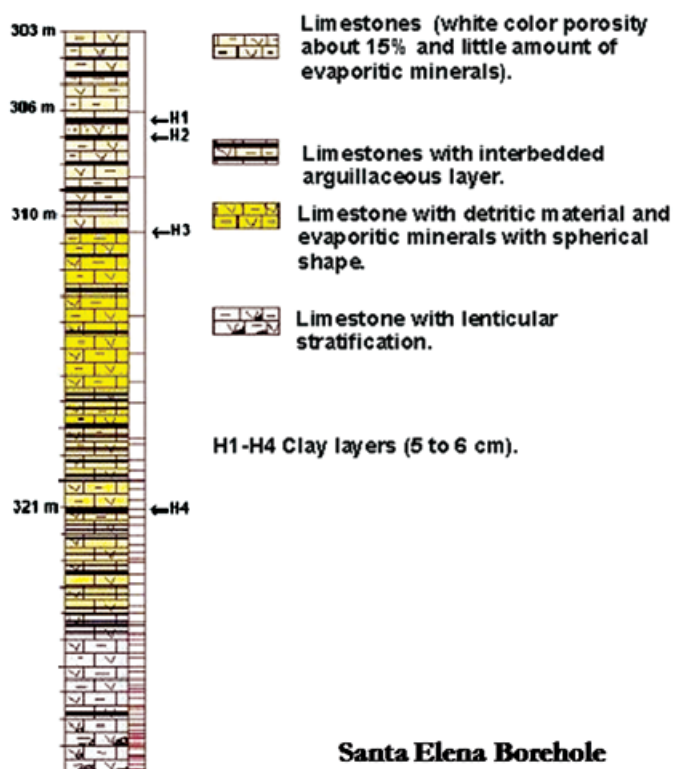


Fig. 2. Lithological column for the basal sequence in the Santa Elena borehole, for the first 30 meters on top of the impact breccia-carbonates contact at about 332 m depth.

Table 1

Geochemical data on the Paleocene carbonate sequence of Santa Elena borehole. Major oxides.

| Sample | Depth (m) | SiO ₂ | TiO ₂ | Al ₂ O ₃ | Fe ₂ O ₃ t | MnO | MgO | CaO | Na ₂ O | K ₂ O | P ₂ O ₅ |
|------------------|-----------|------------------|------------------|--------------------------------|----------------------------------|-------|-------|-------|-------------------|------------------|-------------------------------|
| Standard ES-17Vq | | 9.83 | 0.089 | 2.45 | 0.76 | 0.03 | 5.36 | 40.79 | 0.04 | 1.72 | 0.015 |
| Standard ES-17 | | 10.55 | 0.082 | 2.485 | 0.797 | 0.034 | 5.754 | 41.67 | 0.016 | 1.629 | 0.006 |
| U5-60 | 306.05 | 1.94 | 0.01 | 0.47 | 0.23 | 0.02 | 1.67 | 52.86 | 0.15 | 0.27 | 0.07 |
| U5-50 | 319.62 | 2.50 | 0.02 | 0.54 | 0.31 | 0.02 | 2.71 | 51.57 | 0.13 | 0.34 | 0.05 |
| U5-42 | 322.41 | 1.57 | 0.03 | 0.34 | 0.08 | 0.03 | 1.40 | 52.80 | 0.07 | 0.36 | 0.07 |
| U5-34 | 325.03 | 5.29 | 0.05 | 1.15 | 0.57 | 0.02 | 4.66 | 47.30 | 0.16 | 0.71 | 0.08 |
| U5-26 | 327.26 | 5.50 | 0.05 | 1.25 | 0.63 | 0.04 | 7.25 | 43.87 | 0.14 | 0.73 | 0.17 |
| U5-16 | 329.29 | 6.89 | 0.07 | 1.60 | 0.72 | 0.08 | 9.78 | 39.73 | 0.17 | 0.93 | 0.10 |
| U5-12 | 329.76 | 7.20 | 0.07 | 1.68 | 0.83 | 0.08 | 9.84 | 39.20 | 0.13 | 1.00 | 0.11 |
| U5-5 | 330.9 | 7.73 | 0.09 | 1.82 | 1.13 | 0.13 | 11.08 | 36.60 | 0.13 | 1.16 | 0.11 |
| U5-3 | 331.23 | 7.07 | 0.09 | 1.78 | 1.21 | 0.15 | 11.41 | 37.37 | 0.15 | 1.11 | 0.11 |

Table 2

Geochemical data on the Paleocene carbonate sequence of Santa Elena borehole. Trace elements.

| Sample | Depth (m) | Rb | Sr | Ba | Y | Zr | Nb | V | Cr | Co | Ni | Cu | Zn | Th | Pb |
|------------------|-----------|-------|-------|-------|------|-------|------|------|------|------|------|------|------|------|------|
| Standard ES-17Vq | | 15.16 | 137.0 | 46.88 | 8.91 | 23.98 | 2.19 | 9.60 | 7.28 | 0.98 | 5.37 | 3.64 | 8.88 | 2.96 | 3.54 |
| Standard ES-17 | | 16 | 125 | 35 | 4.5 | 15 | 1.5 | 13.5 | 1.5 | 4.5 | 2 | 5.5 | 8 | 2.5 | 4 |
| U5-60 | 306.05 | 4 | 306 | <11 | <0.7 | 1 | <0.7 | <5 | <2 | <3 | <1 | 5 | 8 | <3 | <4 |
| U5-50 | 319.62 | 4 | 277 | <11 | <0.7 | 2 | <0.7 | 6 | 6 | <3 | 2 | 7 | 8 | <3 | <4 |
| U5-42 | 322.41 | 5 | 259 | <11 | <0.7 | 2 | <0.7 | 9 | 5 | <3 | <1 | 6 | 6 | <3 | <4 |
| U5-34 | 325.03 | 9 | 274 | <11 | <0.7 | 5 | <0.7 | 16 | 12 | 4 | 4 | 8 | 10 | <3 | <4 |
| U5-26 | 327.26 | 8 | 235 | <11 | 1 | 5 | <0.7 | 15 | 9 | 7 | 7 | 9 | 16 | <3 | <4 |
| U5-16 | 329.29 | 9 | 205 | <11 | 1 | 9 | <0.7 | 25 | 18 | 5 | 13 | 12 | 23 | <3 | <4 |
| U5-12 | 329.76 | 9 | 203 | <11 | 1 | 10 | <0.7 | 27 | 21 | 7 | 17 | 12 | 29 | <3 | <4 |
| U5-5 | 330.9 | 10 | 205 | 14 | 1 | 11 | <0.7 | 27 | 20 | 6 | 20 | 13 | 24 | <3 | <4 |
| U5-3 | 331.23 | 9 | 135 | <11 | 2 | 12 | 1 | 32 | 22 | 5 | 21 | 14 | 27 | 3 | <4 |

CaO is a major component, ranging from ~37 to ~53 % wt. Samples above the breccia-carbonates contact are enriched in silica and magnesium, with MgO up to ~11.5 % wt and SiO₂ up to ~8 % wt. All other major oxides show enrichment towards the base of the section. In contrast, samples from levels above 322 m depth present little variation. Major oxides are plotted as a function of stratigraphic position in Figs. 3 and 4. MgO, SiO₂, Al₂O₃, K₂O, FeO and other major oxides are enriched in the basal sediments with a characteristic pattern that inversely correlates with CaO variation (Fig. 3). The high major oxide contents are present in the first 10 m, with the major change in elemental contents observed at 322 m.

The major component in the trace elements is strontium, with concentrations up to 300 ppm. Other trace elements show concentrations of less than 40 ppm. Trace elements are plotted as a function of stratigraphic position in Figs. 5 and 6. Sr shows a similar pattern with stratigraphic position similar to CaO, increasing from 120 ppm at the base to values above 260 ppm at 322 m. Other trace elements, except strontium, show higher contents towards the base of the section, decreasing upwards to 322 m, with little variation in the upper section. The basal sediments show enrichment in trace elements (Zn, V, Cr, Ni, Cu, Zr and Rb).

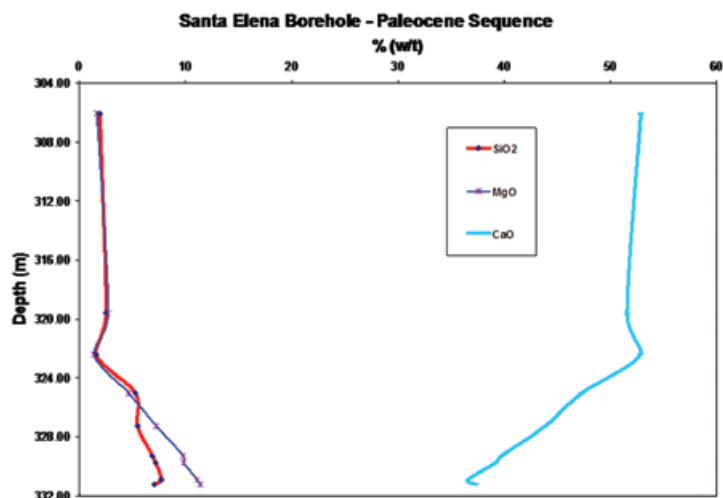


Fig. 3. Major oxide data for the Paleocene sequence in the Santa Elena borehole. Stratigraphic variation of CaO, SiO₂ and MgO with relative position in the core.

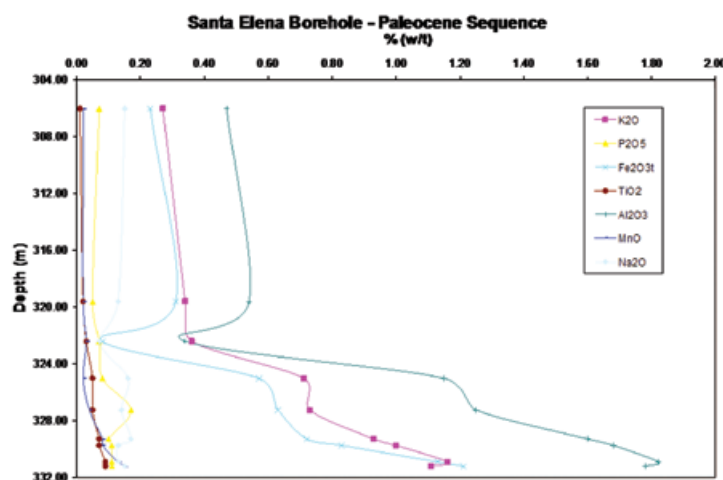


Fig. 4. Major oxide data for the Paleocene sequence in the Santa Elena borehole. Stratigraphic variation of K₂O, P₂O₅, Fe₂O₃, TiO₂, Al₂O₃, MnO and Na₂O with relative position in the core.

Discussion

Study of impact hydrothermal systems provide information on the thermal and chemical evolution and conditions during crater formation, collapse and post-impact processes, including temperature field, metasomatism, fluid circulation, brine sources and composition, weathering and diagenesis. The thermal anomaly in impact craters come from the energy released by impact, deformation and fracturing of target material, crustal excavation and uplift, and the melt sheet and impact breccias. Impacts on marine environments develop convective hydrothermal systems, where seawater, groundwater, formational brines and magmatic fluids circulate. For the Chicxulub crater different estimates

of the volume, extension and location of the melt sheet have been proposed (e.g., Kring, 1995; Ortiz-Aleman and Urrutia-Fucugauchi, 2010). Considering the size and characteristics of the crater, it has been hypothesized that the thermal anomaly lasted for a long time. However, because of the uncertainties in basic crater parameters it is difficult to determine the thermal history for Chicxulub. Furthermore, it has also been difficult to estimate the size and characteristics of the hydrothermal system and the extent of hydrothermal alteration within and outside the crater rim. Most studies have focused on the impactite sequence, characterizing the hydrothermal effects and thermal history (Ames *et al.*, 2004; Kring *et al.*, 2004; Zurcher and Kring, 2004).

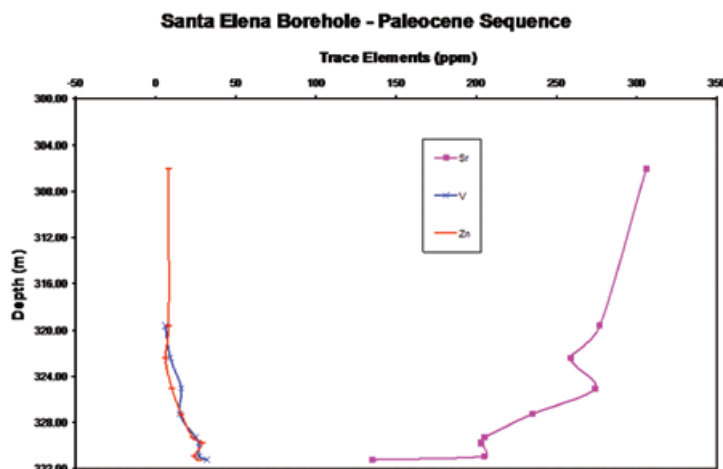


Fig. 5. Trace element data for the Paleocene sequence in the Santa Elena borehole. Data for strontium, vanadium and zinc.

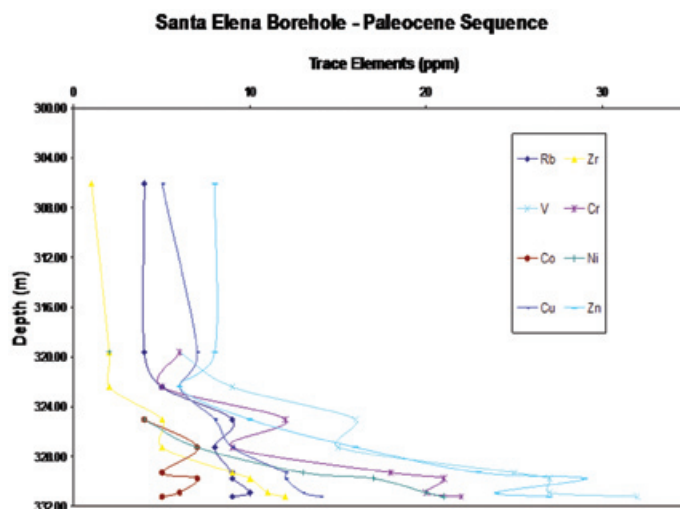


Fig. 6. Trace element data for the Paleocene sequence in the Santa Elena borehole. Data for the Rb, Zr, V, Cr, Co, Ni, Cu and Zn.

In this study, we investigated the hydrothermal activity recorded in the post-impact carbonate sequence deposited in a site immediately outside the main crater rim in the Santa Elena borehole. The influence of the hydrothermal activity is evident in the major oxides and trace element, with a variation pattern in the first 10 m above the impact breccia-carbonates contact (Figs. 3 to 6). The limestones have high concentrations of silica, magnesium, aluminum, potassium and iron, with similar variation patterns in the other oxides. The variation pattern is consistent with the element enrichment associated with hydrothermal effects and less likely resulting from diagenetic processes or decreasing detrital input. The relative contents of the major oxides and trace elements remain constant in the next twelve meters, with CaO around 50 % wt, and SiO₂ and MgO around 2 % wt, suggesting little input and

variation of terrigenous material. Considering the location of the study site outside the crater rim, the geochemical anomalies may arise from convective activity on the underlying impact breccia sequence and input associated with a relatively distal hydrothermal source in the central crater area.

The trace element variation with stratigraphic position is consistent with the pattern for major oxides. Strontium increases from about 120 ppm to 300 ppm (Fig. 5) correlating with the CaO contents, associated with seawater relative input into the carbonates. Trace elements (vanadium, zinc, chromium, nickel, copper, zirconium and rubidium) are enriched in the basal sediments and decrease above the breccia-carbonates contact in the first ten meters (Fig. 6).

Rowe *et al.* (2004) proposed that post-impact activity in the Yaxcopoil-1 Tertiary carbonates resulted from hydrothermal venting into the water column associated with hydrothermal fluids and seawater circulation. In their interpretation, they suggested that fallout of suspended particulate matter from a distal hydrothermal plume produced the high concentrations of manganese, iron, phosphorous, titanium and aluminum observed in the basal 16 m thick carbonate section on top of the impact breccias. Zurcher and Kring (2004) suggested that heat sources within the crater were located towards its center above the thick melt sheet. Zurcher and Kring (2004) studied the impactite section in the Yaxcopoil-1 borehole and concluded that hydrothermal activity evolved from an early Ca-Na-K metasomatic stage to late hydrous stage, with the uppermost impactite section exposed to weathering in subaerial or subaqueous conditions before being covered by the Paleocene carbonates. The hydrothermal system resulted in an early high-temperature (> 300 °C) phase followed by extensive low temperature conditions.

Yaxcopoil-1 borehole is located at about 62 km radial distance from crater center and inside the basin (Urrutia-Fucugauchi *et al.*, 2004a). Compared to the location of the Santa Elena borehole outside the crater rim, hydrothermal input from distal source inside the crater may have been stronger and lasted longer. This is apparently indicated by the geochemical patterns in Yaxcopoil-1 that span ~16 m of the basal sequence. Rowe *et al.* (2004) estimated that hydrothermal activity in the Yaxcopoil-1 zone may have lasted for 300 ka or longer, based on biostratigraphic and magneto-stratigraphic data (Arz *et al.*, 2004; Urrutia-Fucugauchi *et al.*, 2004a). In the case of Santa Elena, magnetic polarity stratigraphy for the basal sequence show that the first ten meters span four polarity chrons from C29r to C28n (Rebolledo-Vieyra and Urrutia-Fucugauchi, 2006) and may represent > 2 Ma. The geochemical pattern in the carbonates shows a systematic decrease in concentration of major oxides and trace elements to background levels (Figs. 3 to 6). Assuming that the source for the particulate matter came from distal locations in the central crater zone where the hydrothermal plumes were injected into the water column, the geochemical patterns indicate a reduction of activity with time. The hydrothermal system may have been active for a shorter period, comparable to estimates in other crater systems. For Sudbury, which is similar in size/morphology to Chicxulub, duration of activity of hydrothermal system is estimated at about 1 Ma (Ames *et al.*, 2004). Active hydrothermal activity in the central zone of Chicxulub may be comparable; although the two structures show significant differences in the volume of the melt sheet. The concentration in Fe, K and Al is suggestive of a step pattern, which is also observed in the trace element data (Zn, V, Cr, Ni, Cu, Zr

and Rb). After cessation of the active hydrothermal stage after ~1 Ma, intermittent hydrothermal venting may have operated for an extended time.

Acknowledgments

We acknowledge comments by the journal reviewers. The study forms part of the UNAM Chicxulub Drilling Program. We thank Rufino Lozano for laboratory analyses and L. Pérez Cruz for collaboration with the study. JEES acknowledges support from CONACYT scholarship grant. The core studies are partly supported by Ixtli Digital Observatory project and DGAPA UNAM PAPIIT IN-114709 grant.

Bibliography

- Ames, D. E., I. M. Kjarsgaard, K. O. Pope, B. Dressler and M. Pilkington, 2004. Secondary alteration of the impactite and mineralization in the basal Tertiary sequence, Yaxcopoil-1, Chicxulub impact crater, Mexico. *Meteoritics and Planetary Science*, 39, 7, 1145-1167.
- Arz, J. A., L. Alegret and I. Arenillas, 2004. Foraminiferal biostratigraphy and paleoenvironmental reconstruction at the Yaxcopoil-1 drill hole, Chicxulub crater, Yucatán Peninsula. *Meteoritics and Planetary Science* 39, 7, 1099-1111.
- Campos-Enriquez, J. O., J. A. Arzate, J. Urrutia-Fucugauchi and O. Delgado-Rodríguez, 1997. The subsurface structure of the Chicxulub crater (Yucatan, Mexico): Preliminary results of a magnetotelluric study. *Leading Edge*, 16, 1774-1777.
- Collins, G. S., J. Morgan, P. Barton, G. L. Christeson, S. Gulick, J. Urrutia-Fucugauchi, M. Warner and K. Wünnemann, 2008. Dynamic modeling suggests terrace zone asymmetry in the Chicxulub crater is caused by target heterogeneity. *Earth and Planetary Science Letters*, 270, 221-230.
- Connors, M., A. R. Hildebrand, M. Pilkington, C. Ortiz-Alemán, R. Chávez, J. Urrutia-Fucugauchi, E. Graniel, A. Camara-Zi, J. Vásquez and J. F. Halpenny, 1996. Yucatan karst features and the size of Chicxulub crater. *Geophysical Journal International*, 127, F11-F14.
- Delgado-Rodríguez, O., J. O. Campos-Enriquez, J. Urrutia-Fucugauchi and J. A. Arzate, 2001. Occam and Bostick 1-D inversion of magnetotelluric soundings in the Chicxulub impact crater, Yucatan, Mexico. *Geofísica Internacional*, 40, 271-283.

- Gulick, S., P. Barton, G. Christeson, J. Morgan, M. MacDonald, K. Mendoza, J. Urrutia-Fucugauchi, P. Vermeesch and M. Warner, 2008. Importance of pre-impact crustal structure for the asymmetry of the Chicxulub impact crater. *Nature Geoscience*, 1, 131-135.
- Hildebrand, A. R., G. T. Penfield, D. A. Kring, M. Pilkington, A. Camargo-Zanoguera, S. B. Jacobsen and W. V. Boynton, 1991. Chicxulub Crater: A possible Cretaceous/Tertiary boundary impact crater on the Yucatan Peninsula, Mexico. *Geology*, 19, 867-871.
- Hildebrand, A., M. Pilkington, C. Ortiz, R. Chavez, J. Urrutia-Fucugauchi, M. Connors, E. Graniel, A. Camara-Zi, J. F. Halpenny and D. Niehaus, 1998. Mapping Chicxulub crater structure with gravity and seismic reflection data. In: *Meteorites: Flux With Time and Impact Effects*, M. M. Graddy, R. Hutchinson, G. J. H. McCall and D. A. Rotherby (Eds.), *Geol. Soc. London Sp. Publ.*, 140, 153-173.
- Kring, D. A., 1995. The dimensions of the Chicxulub impact crater and impact melt sheet. *J. Geophys. Res.*, 100, 16, 979-16, 986.
- Kring, D. A., L. Horz, L. Zurcher and J. Urrutia Fucugauchi, 2004. Impact lithologies and their emplacement in the Chicxulub impact crater: Initial results from the Chicxulub scientific drilling project, Yaxcopoil, Mexico. *Meteoritics and Planetary Science*, 39, 879-897.
- Kring, D. A. and W. B. Boynton, 1992. Petrogenesis of an augite-bearing melt rock in the Chicxulub structure and its relationship to K/T impact spherules in Haiti. *Nature*, 358, 141 - 144. doi:10.1038/358141a0.
- Lopez-Ramos, E., 1976. Geological summary of the Yucatan peninsula. In: *The Ocean Basins and Margins*, Vol. 3, The Gulf of Mexico and the Caribbean, A. E. M. Nairn and F.G. Stehli, Eds., Plenum, New York, 257-282.
- Lozano, R., J. P. Bernal, P. Girón, P. Peñaflor and E. Morales, 2003. Preparación de curvas de calibración para FRX usando la serie IGL como material de referencia. *Actas INAGEQ*, 9, 60-72.
- Melosh, H. J., 1989. *Impact Cratering: A Geologic Process*. Oxford University Press, New York, 245 pp.
- Morgan, J. V., M. R. Warner and the Chicxulub working group, 1997. Size and morphology of the Chicxulub impact crater. *Nature*, 390, 472-476.
- Ortiz-Aleman, C. and J. Urrutia-Fucugauchi, 2010. Aeromagnetic anomaly modeling of central zone structure and magnetic sources in the Chicxulub crater, *Physics of the Earth and Planetary Interiors*, doi:10.1016/j.pepi.2010.01.007.
- Ortiz-Aleman, C., J. Urrutia-Fucugauchi and M. Pilkington, 2001. Three-dimensional modeling of aeromagnetic anomalies over the Chicxulub crater. Lunar Planet. Sci. Conf., XXXII, Houston, Texas, Conference CD Files.
- Penfield, G. T. and A. Camargo-Zanoguera, 1981. Definition of a major igneous zone in the central Yucatán platform with aeromagnetism and gravity, en *Technical Program, Abstracts and Bibliographies, 51st Annual Meeting*, p.37, Society of Exploration Geophysicists, Tulsa, Oklahoma.
- Pilkington, M., D. E. Ames and A. R. Hildebrand, 2004. Magnetic mineralogy of the Yaxcopoil-1 core, Chicxulub. *Meteoritics and Planetary Science*, 39, 6, 831-841.
- Pilkington, M., A. R. Hildebrand and C. Ortiz-Aleman, 1994. Gravity and magnetic field modeling and structure of the Chicxulub crater, Mexico. *J. Geophys. Res.*, 99, 13, 147-13, 162.
- Rebolledo-Vieyra, M., J. Urrutia-Fucugauchi, L. Marin, A. Trejo-Garcia, V. L. Sharpton and A. Soler, 2000. UNAM scientific shallow-drilling program of the Chicxulub impact crater, *Int. Geol. Rev.*, 42, 928-940.
- Rebolledo-Vieyra, M. and J. Urrutia-Fucugauchi, 2006. Magnetostratigraphy of the Cretaceous/Tertiary boundary and Early Paleocene sedimentary sequence from the Chicxulub impact crater. *Earth Planets Space*, 58 10, 1,309-1,314.
- Rowe, A. J., J. J. Wilkinson, B. J. Coles and J. V. Morgan, 2004. Chicxulub: Testing for post-impact hydrothermal input into the Tertiary ocean, *Meteoritics and Planetary Science*, 39, 7, 1223-1231.
- Salguero-Hernandez, E., J. Urrutia-Fucugauchi, and L. Ramirez-Cruz, 2010. **Fracturing and deformation in the Chicxulub crater – Complex trace analysis of instantaneous seismic attributes.** *Revista Mexicana de Ciencias Geologicas*, in press.
- Sharpton, V. L., G. Dalrymple, L. Marin, G. Ryder, B. Schuraytz and J. Urrutia-Fucugauchi, 1992. New links between the Chicxulub impact structure and the Cretaceous/Tertiary boundary. *Nature*, 359, 819-821.

Sharpton, V. L., K. Burke, A. Camargo, S. A. Hall, S. Lee, L. Marin, G. Suarez, J. M. Quezada, P. D. Spudis and J. Urrutia-Fucugauchi, 1993. Chicxulub multiring impact basin: Size and other characteristics derived from gravity analysis. *Science*, 261, 1,564-1,567.

Urrutia-Fucugauchi, J. and L. Perez-Cruz, 2007. Deep drilling into the Chicxulub impact crater: Pemex oil exploration boreholes revisited. American Geophysical Union Joint Assembly, CD Program & Abstracts U33A-07.

Urrutia-Fucugauchi, J. and L. Perez-Cruz, 2009. Multiring-forming large bolide impacts and evolution of planetary surfaces. *International Geology Review*, 51, 1079-1102. doi: 10.1080/00206810902867161.

Urrutia-Fucugauchi, J., L. Marin and A. Trejo-Garcia, 1996. UNAM scientific drilling program of Chicxulub impact structure: Evidence of a 300-km crater diameter, *Geophys. Res. Lett.*, 23, 1,565-1,568.

Urrutia-Fucugauchi, J., J. Morgan, D. Stoeffler and P. Claeys, 2004a. The Chicxulub Scientific Drilling Project. *Meteoritics and Planetary Science*, 39, 787-790.

Urrutia-Fucugauchi, J., A. Soler, M. Rebolledo-Vieyra and P. Vera, 2004b. Paleomagnetic and rock magnetic study of the Yaxcopoil-1 impact breccia sequence, Chicxulub impact crater, Mexico. *Meteoritics and Planetary Science*, 39, 843-856.

Urrutia-Fucugauchi, J., J. M. Chavez-Aguirre, L. Perez-Cruz and J. L. de la Rosa, 2008. Impact ejecta and carbonate sequence in the eastern sector of Chicxulub crater. *Comptes Rendus Geosciences*, 341, 801-810.

Zurcher, L. and D. A. Kring, 2004. Hydrothermal alteration in the Yaxcopoil-1 borehole, Chicxulub impact structure, Mexico. *Meteoritics and Planetary Science*, 39, 1199-12.

J. E. Escobar-Sanchez*, J. Urrutia-Fucugauchi
Proyecto Universitario de Perforaciones en Océanos
y Continentes, Laboratorio de Paleomagnetismo y
Paleoambientes, Instituto de Geofísica, Universidad
Nacional Autónoma de México, Ciudad Universitaria,
Del. Coyoacán, 04510, Mexico City, Mexico
*Corresponding author: elia@geofisica.unam.mx